

Fetal ECG Extraction on Time-Frequency Domain using Conditional GAN

Vuong D. Nguyen

Quantitative Imaging Lab, University of Houston

dnguy222@cougarnet.uh.edu

Abstract

Fetal electrocardiogram (ECG) analysis plays an important role in assessing fetal heart rate, rhythm, and detecting potential cardiac anomalies. However, obtaining fetal ECG remains challenging due to its inherently low amplitude and susceptibility to maternal signal interference. In this paper, we propose a novel approach for robust fetal ECG extraction using a Conditional Generative Adversarial Network (cGAN) that operate on time-frequency domain of abdominal ECG signals instead of raw 1D abdominal ECG signals. By utilizing the frequency domain, our model is able to capture intricate time-varying patterns often obscured by noise and interference in the time domain. Moreover, cGAN leverages prior knowledge about fECG signal structures, enhancing the accuracy of fECG reconstruction. Experimentations on real-world ECG dataset validates the efficacy of our model in accurately extracting fECG signals, achieving high structural similarity score (SSIM) and low mean squared error (MSE) when compared with corresponding ground truth test sets. The approach shows superiority over conventional methods, demonstrating robustness to noise and interference. All in all, this work presents a promising avenue for advancing non-invasive fECG extraction techniques and its potential applications in clinical settings.

1. Introduction

Monitoring fetal health during pregnancy is of utmost importance to ensure a safe delivery and healthy newborn. One way of assessing fetal well-being is by analyzing the fetal electrocardiogram (fECG) signal [5] which provides essential insights into fetal heart rate, rhythm, and cardiac anomalies, enabling early intervention and improved outcomes. However, obtaining fECG signals can be challenging due to its low amplitude and interference from maternal abdominal signals [29]. Directly measuring the fECG signal using invasive procedures is often expensive, uncomfortable, and can pose risks to both the mother and the fetus [26, 32]. Non-invasive fetal ECG extraction is the process of sepa-

rating the fECG signal from the abdominal ECG (aECG) signal recorded from the abdominal surface of a pregnant woman [29]. But these methods are challenging due to signal interference [8], noise [2] [3], as well as differing morphologies of the recordings.

Numerous studies have explored adaptive filtering techniques, such as Independent Component Analysis (ICA) [17, 21, 30] and Template subtraction (TS) [1, 23], to separate fECG from mECG signals. However, these methods often encounter convergence issues, lack precision, and rely on knowledge of maternal QRS (mQRS) locations, which can be unavailable. Deep learning-based (DL) approaches, as seen in fetal QRS detection, offer promise for fECG extraction tasks even without mECG signals. DL enables end-to-end processing, but prior AutoEncoder-based attempts depended on extensive preprocessing and hyperparameter tuning. Previous work mainly focused on raw 1-D data, necessitating complex preprocessing for competitive performance.

In this paper, we argue that transforming ECG data into time-frequency domain is more effective in terms of preprocessing effort and especially accuracy of fECG extraction. Specifically, short-time Fourier Transform is utilized to obtain time-frequency representations of ECG data in the form of spectrograms. We design a novel framework based on Conditional Generative Adversarial Network (cGAN) [18] whose input are spectrograms of aECG signals, and the model attempts to reconstruct spectrograms of fECG signals as outputs. To achieve this, the model consists of an attention-based generator and a discriminator that work in an adversarial manner. By conditioning both generator and discriminator with ground truths spectrograms of fECG signals, the generator attempts to learn to generate spectrograms of fECG signals from aECG spectrograms while the discriminator tries to distinguish between these spectrograms and ground truth spectrograms.

This approach is well-suited to our task because it can effectively capture complex time-frequency patterns in the ECG signals, which are often difficult to extract using traditional signal processing techniques. Furthermore, the ability to incorporate prior knowledge about the expected struc-

ture of fECG signals into the cGAN model allows for more accurate reconstruction of fECG signals from aECG inputs. As far as we are concerned, this paper is the first work that proposes to perform fECG extraction using cGAN on time-frequency domain.

Overall, the main contributions of this paper are as follows:

1. Providing insights into the time-frequency characteristics of fetal and mECG signals and how they can be exploited for more accurate fECG extraction.
2. Proposing a novel approach for fECG extraction on the time-frequency domain using Conditional GAN, which has not been explored in previous studies.
3. Evaluating the effectiveness of our method using a real-world dataset, and comparing the results with conventional methods.

2. Related Work

Conventional fECG extraction methods encompass Adaptive Filtering, Blind Source Separation (BSS), and Template Subtraction (TS). Adaptive algorithms in previous works [16, 25] address noise and interference in abdominal signals, yet necessitate prior knowledge and are susceptible to noise artifacts. BSS techniques [17, 21, 30] assume independence among sources, which is not always practical for device implementation. TS [1, 23] utilizes maternal ECG templates for removal, but its effectiveness varies with mECG variability and fECG strength.

Deep Learning has been extensively studied in signal data especially ECG signals because of its ability to learn and extract features automatically. A deep learning approach in Zhong *et al.* [31] employs a 1-D CNN to detect fetal QRS (fQRS) complexes, inspiring subsequent work on fQRS detection like Lee *et al.* [13] and Huque *et al.* [9]. Mirza *et al.* [19] utilize fQRS as references to locate fetal ECG signals in raw aECG data, using a ResNet-based model with 1-D octave convolution. Lo *et al.* [15] adopt a 2-D CNN for fECG extraction, treating it as a four-class classification task. However, these CNN-based methods require large amounts of training data to achieve high accuracy and may not be effective in cases where the fetal ECG is weak and the signal to noise ratio (SNR) is low.

Recent work has focused on using AutoEncoders (AEs) for fetal ECG extraction which are neural networks trained to reconstruct the input data. For instance, [20] proposed an AE-based method to reconstruct fECG signals by stacking Denoising AEs. This is followed by a residual U-net convolutional encoder-decoder network proposed in [33]. AECG-DecomposeNet in [27] has extended this approach by utilizing two U-net architectures in series, one for extracting mECG signals and other for removing them from the maternal-abdominal ECG. Nevertheless, these methods have limitations in removing mECG signals accurately

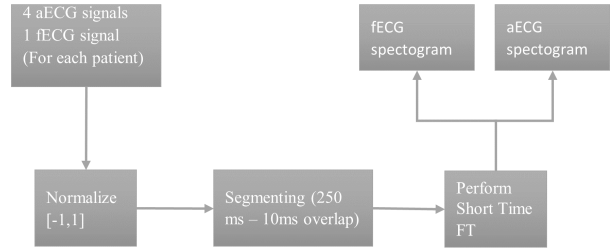


Figure 1. Spectrogram generation module: Takes the 1D aECG and fECG signals as input, then generates 2D spectrograms.

when the amplitudes of the fetal and maternal ECG signals are similar. The work in [4] builds a multi-channel fECG denoising using convolutional AE by assuming the mECG pattern is provided and can be easily removed from aECG signals. W-Net, where two U-net are stacked, is designed by Jin *et al.* [14] to separate maternal and fetal ECG. However this architecture requires large computing resources and is not efficient in practical scenarios. Moreover, these techniques require large amount labelled fECG signal as references, while labelled fECG data is very limited and hard to collect by non-invasive methods.

3. Dataset

The Abdominal and Direct Fetal ECG Database (A&DFECG) [6] from PhysioNet is a collection of ECG recordings of abdominal and direct fetal ECG signals from five pregnant women. Each recording consists of four abdominal channels and one direct fetal channel, all are 5-minute long. The signals were sampled at a rate of 1 kHz and 16-bit resolution. We use this database as the training dataset by making use of direct fECG signal channel as target domain of our proposed cGAN model, while the four abdominal channels act as the input domain of the model.

4. Methodology

The overview of our proposed framework is depicted in Figure 2. First the 1D aECG and their corresponding fECG signals are passed to the spectrogram generation module that performs Fourier transform to obtain the 2D time-frequency representations. The generated aECG and fECG spectrograms serve as input to the cGAN module which learns to synthesize the fECG spectrograms from aECG spectrograms. Output of cGAN module are then compared with the ground truth fECG spectrograms using the evaluation module.

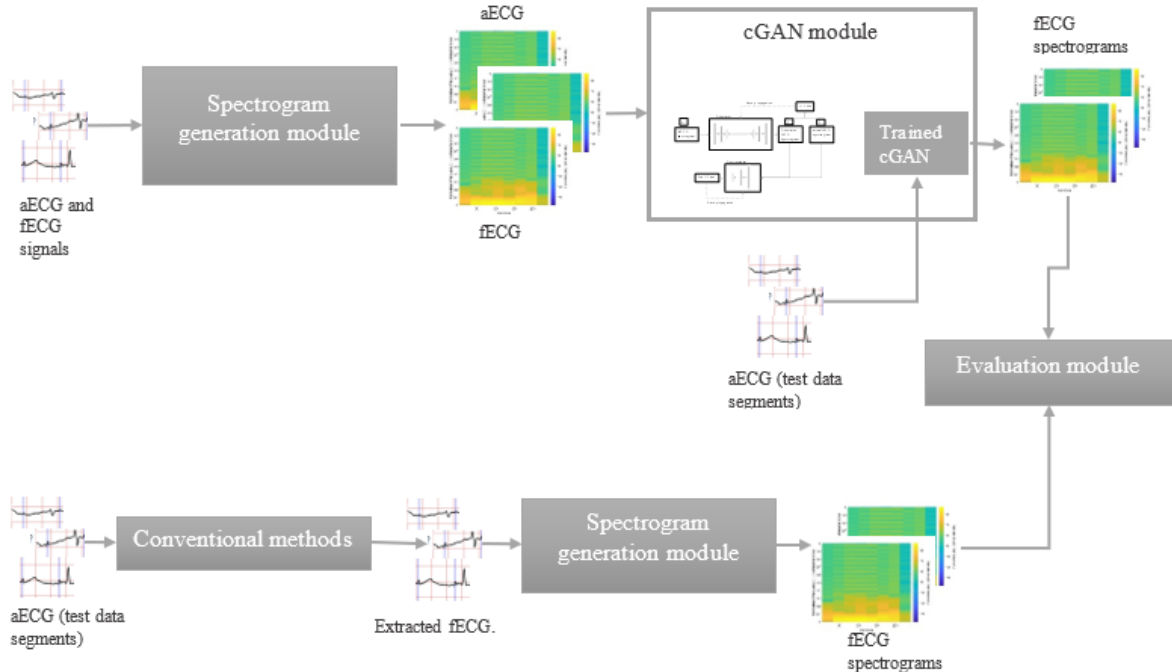


Figure 2. Overall framework: There are three main modules: (1) spectrogram generation module that performs Fourier transform on 1D signals to obtain the 2D time-frequency representations (2) cGAN module that comprises a cGAN to synthesize the fECG spectrograms from aECG spectrograms; and (3) the evaluation module that evaluates the performance of our method for fECG extraction.

4.1. Time-Frequency Representations

In signal processing, Fourier analysis is a prevalent technique known for its ability to reveal frequency domain properties. However, it's unable to precisely pinpoint the timing of events, making it particularly challenging when confronted with time-varying signals like those found in fECG data. To address this, the Short Time Fourier Transform (STFT), often referred to as the windowed Fourier Transform, emerges as a pivotal tool in delivering essential information about both the timing and frequency of signal events. This precise localization is contingent upon the size of the window used in the transformation. In the context of fetal health monitoring, STFT's application offers a nuanced understanding of fECG signals, aiding in the detection of fetal heart rate, rhythm, and cardiac anomalies. Alongside techniques like the Wavelet Transform, STFT plays a crucial role in the fECG analysis. The STFT equation can be given as

$$F(\tau, \omega) = \int_{-\infty}^{\infty} f(t) \cdot W(t - \tau) \cdot e^{-j\omega t} dt \quad (1)$$

where $w(t - \tau)$ is a window function (often a Hamming window) used to select a specific time segment of the signal.

The dataset includes 1D signals corresponding to four aECG signals and one corresponding fECG signal for each

patient. The process of transforming the 1-1 signals onto time-frequency domain is visually depicted in Figure 1. The signals are first normalized to range $[-1, 1]$. Following normalization, the signals are segmented into discrete intervals of 250ms duration, with overlapping segments of 10ms. This segmentation strategy enhances the dataset's input diversity for deep learning networks and facilitates comprehensive signal analysis. Subsequently, STFT is applied to these signal segments to obtain fECG and aECG spectrograms. Note that four spectrograms from four distinct aECG channels are associated with a single fECG spectrogram label.

4.2. Conditional GAN Module

On time-frequency domain, in this work, we propose to leverage Conditional GAN (cGAN) [18] to translate aECG spectrograms to fECG spectrograms as illustrated in Figure 3. cGAN is an extension of GAN [7]. Given a random noise vector z , GAN learns a generator \mathcal{G} to output image y : $\mathcal{G} : z \rightarrow \hat{y}$. On the other hand, a discriminator \mathcal{D} is tasked with distinguishing between real image y and generated images \hat{y} . In an adversarial manner, the generator \mathcal{G} is trained to generate images that can fool the discriminator \mathcal{D} . The

objective of a GAN can be stated as:

$$\min_{\mathcal{G}} \max_{\mathcal{D}} (\mathbb{E}_{\hat{y} \sim p(\hat{y})} [\log \mathcal{D}(\hat{y})] + \mathbb{E}_{z \sim p_z(z)} [\log (1 - \mathcal{D}(\mathcal{G}(z)))]). \quad (2)$$

Different from GAN, the generator \mathcal{G}_C of cGAN maps an observed aECG spectrogram x and random noise vector z to output fECG spectrogram image \hat{y} : $\mathcal{G}_C : \{x, z\} \rightarrow \hat{y}$. The discriminator \mathcal{D}_C is trained to detect as well as possible if the generated fECG spectrogram \hat{y} is real or fake using the objective function conditioning on x :

$$\mathcal{L}(\mathcal{D}_C) = \mathbb{E}_{x, z} [\log (1 - \mathcal{D}_C(x, \mathcal{G}_C(x, z)))] . \quad (3)$$

The objective of \mathcal{G}_C becomes minimizing the ability of \mathcal{D}_C to distinguish between x and \hat{y} :

$$\mathcal{L}(\mathcal{G}_C) = \mathbb{E}_{x, \hat{y}} [\log (\mathcal{D}(x, \hat{y}))] . \quad (4)$$

Besides fooling the discriminator, the generator is constrained to output images that are near the ground truth images based on L1 distance:

$$\mathcal{L}_{L1}(\mathcal{G}_C) = \mathbb{E}_{x, y, z} [\|y - \mathcal{G}_C(x, z)\|_1] . \quad (5)$$

The final loss of the cGAN model can be summarized as:

$$\mathcal{L}_{cGAN} = \mathcal{L}(\mathcal{G}_C) + (-\mathcal{L}(\mathcal{D}_C)) + \mathcal{L}_{L1}(\mathcal{G}_C) . \quad (6)$$

The architectures of the generator and discriminator use modules of the form convolution-BatchNorm-ReLu, which are adapted from [10, 24]. Since aECG spectrograms to fECG spectrograms share a great deal of low-level information, for the generator, we follow the general shape of a U-Net [28] with N layers. Then we add skip connections that concatenates all channels at each layer k with those at layer $N - k$.

4.3. Evaluation Module

Figure 4 shows the main steps of the evaluation module. To validate the effectiveness of our method, we propose a conventional method called Probabilistic Averaging (PA) and perform comparison between the outputs of our framework and PA. For PA, we extract fECG signals based on a series of Gaussian laws. First, to preprocess the signals, we perform a normalization and alignment using QRS annotation. After aligning the signal segments, an array of Gaussian estimators are generated by calculating the means and standard deviations of points grouped by index:

$$\sigma = \frac{\sqrt{\sum x_{ij} - \mu_j}}{N}, \mu_j = \frac{\sum x_i}{N} \quad (7)$$

This yields a generator array capable of accepting any seed and positioning new synthetic segments in acceptable intervals. Finally, random seeds and a random variable were generated to obtain a synthetic signal.

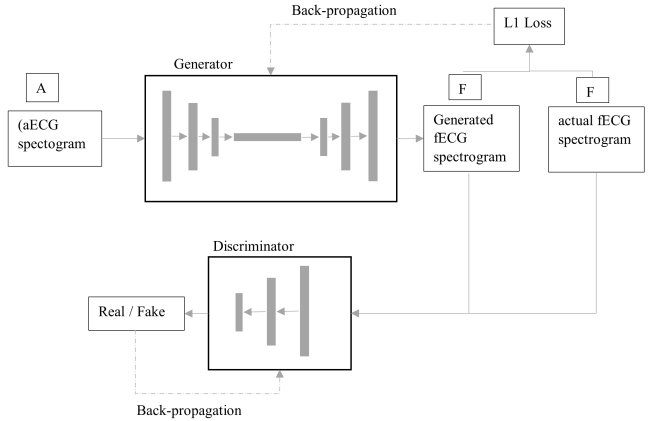


Figure 3. Conditional GAN module: Takes the fECG and aECG spectrograms as input, learns to synthesize fECG spectrograms from the aECG spectrograms.

Two main metrics are used, namely Structural Similarity Index (SSIM) and Mean Squared Error (MSE). SSIM is used to measure the similarity between two images, which is sensitive to changes in structural information. SSIM values range from -1 to 1, with 1 indicating perfect similarity between the images:

$$SSIM(x, y) = \frac{(2\mu_x\mu_y + c_1)(2\sigma_{xy} + c_2)}{(\mu_x^2 + \mu_y^2 + c_1)(\sigma_x^2 + \sigma_y^2 + c_2)}, \quad (8)$$

where μ_x and μ_y , σ_x^2 and σ_y^2 , and σ_{xy} are the mean values, variances, and covariance between images x and y , respectively and c_1 and c_2 are constants. MSE measures the pixel-wise difference between two images. A low MSE value indicates that the images are more similar:

$$MSE = \frac{1}{mn} \sum_{i=0}^{m-1} \sum_{j=0}^{n-1} [I(i, j) - K(i, j)]^2 \quad (9)$$

where MSE represents the Mean Squared Error between two images I and K , where m and n are the dimensions of the images. Using them these two metrics provide us with a complete assessment of quality degradation of the generated spectrograms and help us analyze the errors.

5. Experimental Setup

We leveraged Pix2Pix GAN [11] as the backbone Conditional GAN. The Pix2Pix GAN is implemented with a U-Net generator and a CNN discriminator. The model was trained with a batch size of 16 for 125 epochs. Both the generator and discriminator were trained using Adam [12] optimizer with a learning rate of 0.0002, beta parameters of (0.5, 0.999), weight decay of 0.0001 and momentum of 0.9.

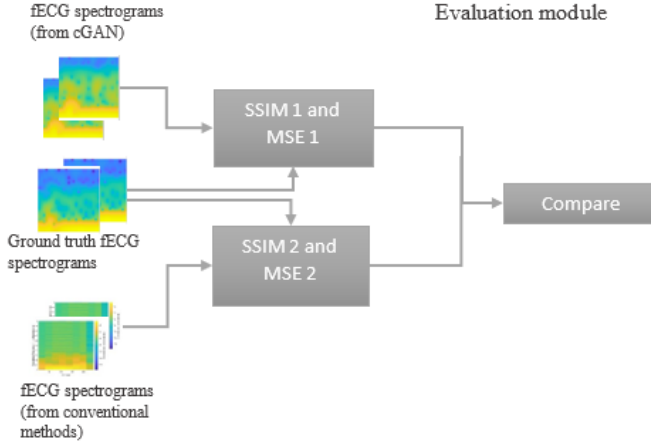


Figure 4. Evaluation module that compares the generated fECG spectrograms with ground truth using MSE and SSIM metrics.

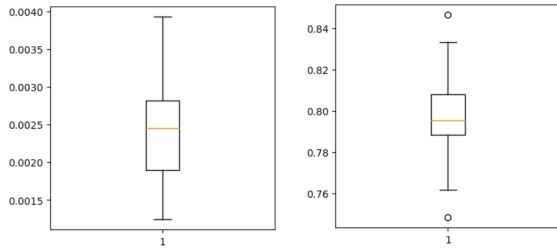


Figure 5. Distribution of MSE values (left) and SSIM values (right) of all pairs of fECG spectrograms generated by our proposed framework from the aECG spectrograms in the test set and its corresponding ground truth fECG spectrograms. MSE Mean: 0.002, MSE Standard deviation: 0.0008; SSIM Mean: 0.801, SSIM Standard deviation: 0.0190.

We reduce the learning rate linearly by a factor of 0.1 after every 50 epochs. Training was performed on a NVIDIA GeForce GTX 1080Ti GPU with 16GB RAM, which took around 16 hours. Implementation is in PyTorch [22].

6. Results

6.1. Overall results

We evaluate the performance of our proposed method on the A&DFECG Database. We quantify the performance of our method using boxplots that show the distribution of MSE and SSIM values for all pairs of aECG and fECG spectrograms in the test set. From Figure 5, the boxplot of MSE values shows a small mean of 0.002 and a low standard deviation of 0.0008, demonstrating that the generated fECG spectrograms are highly accurate in terms of pixel-wise comparison. Similarly, the SSIM values also indicate a high degree of similarity in structure between the generated

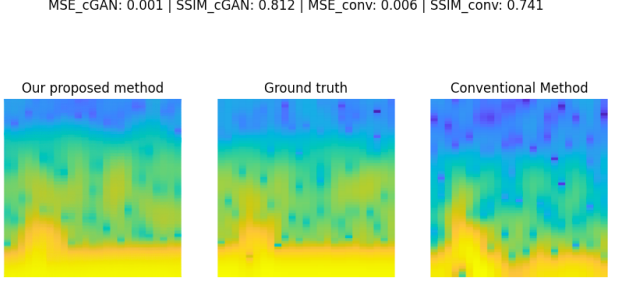


Figure 6. Comparison between fECG spectrograms generated by our proposed method and Probabilistic Averaging. By visual observation, our framework produces more accurate fECG signals and fQRS peaks, which are close to ground truth. In terms of qualitative comparison, our proposed method results in a lower MSE value (0.001 compared to 0.006) and a higher SSIM value (0.812 compared to 0.741).

and ground truth spectrograms, with the mean SSIM value of 0.801 and standard deviation of 0.0190. High level of structural and pixel-wise similarity indicates that the generated fECG spectrograms are close to the ground truth, which demonstrates the effectiveness and accuracy of our proposed method for fECG extraction task.

6.2. Comparison with conventional method

Experiments using Probabilistic Averaging (PA) are conducted to further validate the effectiveness of our method. We take the same test set of 1D aECG signals to generate the 1D fECG which are then converted to their time-frequency representations through the spectrogram generation module and passed to the evaluation module to compare with the ground truth. PA is used to extract fECG signal from aECG signal, which is then segmented and projected onto time-frequency domain to generate spectrograms.

Figure 6 shows the qualitative comparison between outputs of our proposed method and PA with the ground truth fECG spectrograms on a sample segment in the test set. From visual observation, it can be seen that the fECG spectrogram generated by our method is closer to ground truth than that extracted by PA. In terms of metrics, our method produces an MSE value of 0.001, which is significantly lower than that of the conventional method (0.006). Moreover, the SSIM value of our proposed method is higher than that of PA.

We also report the distribution of MSE and SSIM values (Figure 7) of all pairs of fECG spectrograms generated by PA from the aECG segments in the test set. The results indicate that our proposed GAN-based method outperforms PA in terms of both MSE and SSIM values. Specifically, the mean MSE value produced by PA is 0.006 while the mean MSE value produced by our proposed method is 0.002. The mean SSIM value is 0.736, while the mean SSIM value pro-

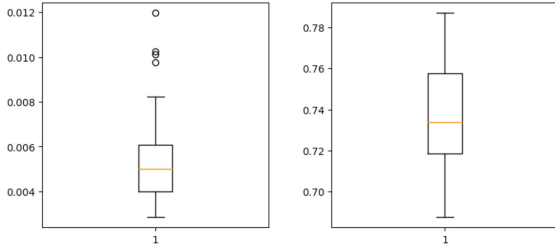


Figure 7. Distribution of MSE values (left) and SSIM values (right) of all pairs of fECG spectrograms produced by Probabilistic Averaging from the aECG segments in the test set. MSE Mean: 0.006, MSE Standard deviation: 0.002; SSIM Mean: 0.736, MSE Standard deviation: 0.026.

duced by our proposed method is 0.801. These results indicate that PA produces fECG spectrograms with a higher degree of error compared to our proposed method, since PA is sensitive to noise artifacts as the noise either skews the mean or widens the standard deviation hence, outliers appear in the signal.

Overall, our proposed model is able to generate higher quality fECG signals compared to the Probabilistic Averaging method, especially when the aECG signal contains a high level of noise or artifacts. Additionally, the Pix2Pix GAN model is able to capture the underlying nonlinear and complex relationships between the aECG and fECG signals, which makes it more robust to changes in the input data compared to the Probabilistic Averaging method.

6.3. Further Analysis

In our work, by segmenting the signal by length of 250ms with an overlap of 10ms and applying STFT in logarithmic scale, we are able to track the power spectral density (PSD) of the signal, and its changes across the time and frequency domains. We used a hamming window to curb the noise and emphasize the QRS sequence, yielding a better depiction of high PSD change in the spectrogram. We also fixed NFFT to 256 to widen the spectrogram sliding window allowing a smooth PSD. This enables the cGAN models to learn from distinctive patterns within the spectrogram as the mECG and fECG are periodic signals and showcase change through time for specific frequency ranges. Those frequencies are characteristics of the PQRS waves. The influence of some multiplicative noise artifacts make the occurrence of these waves pseudo-periodic rather than periodic. The origin of the noise can be linked to multiple artifacts such as equipment, the influence of the mother's movements and other types of vibrations on the fECG. Most of these noises are of additive nature and only affect the amplitude of the ECG signal, influencing the power changes on a quadratic scale.

7. Conclusion

In this paper, we have presented a novel approach for robust fetal ECG extraction using Conditional GAN. Our proposed method utilizes frequency-domain representations of abdominal ECG and fetal ECG signals, which are fed to the Pix2Pix GAN model for generating high-quality fECG spectrograms. We have demonstrated the effectiveness of our approach on the Abdominal and Direct Fetal ECG Database, showing that our method outperforms the conventional method in terms of both quantitative metrics (MSE and SSIM) and visual quality. Our method produces fECG spectrograms with a lower MSE value and a higher SSIM value compared to Probabilistic Averaging method. Future work can explore the use of our approach in combination with other machine learning techniques for further improving the accuracy and reliability of fECG extraction. In conclusion, our proposed method represents a promising direction for robust fetal ECG extraction and has the potential to make a significant impact on the field of fetal health monitoring.

References

- [1] Joachim Behar, Julien Oster, and Gari D Clifford. Combining and benchmarking methods of foetal ECG extraction without maternal or scalp electrode data. *Physiological Measurement*, 35(8):1569–1589, 2014. [1](#) [2](#)
- [2] Gari D. Clifford. *ECG Statistics, Noise, Artifacts, and Missing Data*, chapter 3. Artech House, 2006. [1](#)
- [3] ER Ferrara and B Widrow. Fetal electrocardiogram enhancement by time-sequenced adaptive filtering. *IEEE Transactions on Biomedical Engineering*, 29(6):458–460, 1982. [1](#)
- [4] Eleni Fotiadou, Tomasz Konopczyński, Jürgen Hesser, and Rik Vullings. End-to-end trained encoder-decoder convolutional neural network for fetal electrocardiogram signal denoising. *Physiological Measurement*, 41(1):015005, 2020. [2](#)
- [5] Suzanne M Gilboa et al. Congenital heart defects in the united states: Estimating the magnitude of the affected population in 2010. *Circulation*, 134(2):101–109, 2016. [1](#)
- [6] AL Goldberger, LAN Amaral, L Glass, JM Hausdorff, P Ch Ivanov, RG Mark, JE Mietus, GB Moody, CK Peng, HE Stanley, et al. Physionet: Components of a new research resource for complex physiologic signals. *circ.* 101 (23): e215–e220//circulation electronic pages. 2000. june 13. [2](#)
- [7] Ian J. Goodfellow et al. Generative adversarial networks, 2014. [3](#)
- [8] M A Hasan, M B I Reaz, M I Ibrahimy, M S Hussain, and J Uddin. Detection and processing techniques of FECG signal for fetal monitoring. *Biological Procedures Online*, 11(1): 263–295, 2009. [1](#)
- [9] A.S.A. Huque, K.I. Ahmed, M.A. Mukit, and R. Mostafa. Hmm-based supervised machine learning framework for the detection of fecn r-r peak locations. *Innovation and Research in BioMedical engineering*, 40(3):157–166, 2019. [2](#)
- [10] Sergey Ioffe and Christian Szegedy. Batch normalization: Accelerating deep network training by reducing internal covariate shift, 2015. [4](#)

[11] Phillip Isola, Jun-Yan Zhu, Tinghui Zhou, and Alexei A Efros. Image-to-image translation with conditional adversarial networks. In *Proceedings of the IEEE conference on computer vision and pattern recognition*, pages 1125–1134, 2017. 4

[12] Diederik P. Kingma and Jimmy Ba. Adam: A method for stochastic optimization, 2017. 4

[13] Jun Seong Lee, Minseok Seo, Sang Woo Kim, and Minho Choi. Fetal qrs detection based on convolutional neural networks in noninvasive fetal electrocardiogram. In *2018 4th International Conference on Frontiers of Signal Processing*, pages 75–78, 2018. 2

[14] Kwang Jin Lee and Boreom Lee. End-to-end deep learning architecture for separating maternal and fetal ecgs using w-net. *IEEE Access*, 10:39782–39788, 2022. 2

[15] Fang-Wen Lo and Pei-Yun Tsai. Deep learning for detection of fetal ecg from multi-channel abdominal leads. In *2018 Asia-Pacific Signal and Information Processing Association Annual Summit and Conference*, pages 1397–1401, 2018. 2

[16] Radek Martinek, Petr others, Jan Zidek, Jan Nedoma, and Marcel Fajkus. Non-invasive fetal monitoring: A maternal surface ECG electrode placement-based novel approach for optimization of adaptive filter control parameters using the LMS and RLS algorithms. *Sensors (Basel)*, 17(5), 2017. 2

[17] Radek Martinek, , et al. Comparative effectiveness of ICA and PCA in extraction of fetal ECG from abdominal signals: Toward non-invasive fetal monitoring. *Frontiers in Physiology*, 9:648, 2018. 1, 2

[18] Mehdi Mirza and Simon Osindero. Conditional generative adversarial nets. *arXiv preprint arXiv:1411.1784*, 2014. 1, 3

[19] Sarfaraj Mirza, Kalyani Bhole, and Prateek Singh. Fetal ecg extraction and qrs detection using independent component analysis. In *2020 16th IEEE International Colloquium on Signal Processing and Its Applications (CSPA)*, pages 157–161, 2020. 2

[20] Priya Ranjan Muduli, Rakesh Reddy Gunukula, and Anirban Mukherjee. A deep learning approach to fetal-ecg signal reconstruction. In *2016 Twenty Second National Conference on Communication (NCC)*, pages 1–6, 2016. 2

[21] Sonal Nikam and Shankar Deosarkar. Fast ica based technique for non-invasive fetal ecg extraction. In *2016 Conference on Advances in Signal Processing*, pages 60–65, 2016. 1, 2

[22] Adam Paszke et al. Pytorch: An imperative style, high-performance deep learning library, 2019. 5

[23] Piotr Podziemski and Jan Gieraltowski. Fetal heart rate discovery: Algorithm for detection of fetal heart rate from noisy, noninvasive fetal ecg recordings. *Computing in Cardiology 2013*, pages 333–336, 2013. 1, 2

[24] Alec Radford, Luke Metz, and Soumith Chintala. Unsupervised representation learning with deep convolutional generative adversarial networks, 2016. 4

[25] B. Rafaely and S.J. Elliot. A computationally efficient frequency-domain lms algorithm with constraints on the adaptive filter. *IEEE Transactions on Signal Processing*, 48 (6):1649–1655, 2000. 2

[26] Boaz Rafaely and Stephen J Elliot. A computationally efficient frequency-domain lms algorithm with constraints on the adaptive filter. *IEEE Transactions on Signal Processing*, 48(6):1649–1655, 2000. 1

[27] Arash Rasti-Meymandi and Aboozar Ghaffari. AECG-DecompNet: abdominal ECG signal decomposition through deep-learning model. *Physiological Measurement*, 42(4):045002, 2021. 2

[28] Olaf Ronneberger, Philipp Fischer, and Thomas Brox. U-net: Convolutional networks for biomedical image segmentation, 2015. 4

[29] Zdenek Slanina et al. Fetal phonocardiography signal processing from abdominal records by non-adaptive methods. In *Photonics Applications in Astronomy, Communications, Industry, and High-Energy Physics Experiments*, page 118, 2018. 1

[30] Qiong Yu et al. Automatic identifying of maternal ecg source when applying ica in fetal ecg extraction. *Biocybernetics and Biomedical Engineering*, 38(3):448–455, 2018. 1, 2

[31] Wei Zhong, Lijuan Liao, Xuemei Guo, and Guoli Wang. A deep learning approach for fetal QRS complex detection. *Physiological Measurement*, 39(4):045004, 2018. 2

[32] Wei Zhong, Lijuan Liao, Xuemei Guo, and Guoli Wang. A deep learning approach for fetal qrs complex detection. *Physiological measurement*, 39(4):045004, 2018. 1

[33] Wei Zhong, Lijuan Liao, Xuemei Guo, and Guoli Wang. Fetal electrocardiography extraction with residual convolutional encoder-decoder networks. *Australasian College of Physical Scientists and Engineers in Medicine*, 42(4):1081–1089, 2019. 2